Energy Conversion and Management 196 (2019) 69–76

Contents lists available at ScienceDirect

Energy Conversion and Management

journal homepage: www.elsevier.com/locate/enconman

High-performance terrestrial solar thermoelectric generators without optical concentration for residential and commercial rooftops

Song Lv[a,d], Wei He[a,*], Zhongting Hu[a], Minghou Liu[b], Minghui Qin[c], Sheng Shen[d], Wei Gong[d]

[a] Department of Building Environment and Equipment, Hefei University of Technology, Hefei 230009, China
[b] Department of Thermal Science and Energy Engineering, University of Science and Technology of China, Hefei 230026, China
[c] Department of Architecture and Civil Engineering, Qinghai College of Architectural Technology, Xining, Qinghai 810012, China
[d] Department of Mechanical Engineering, Carnegie Mellon University, Pittsburgh, PA 15213, United States

ARTICLE INFO

Keywords:
Solar thermoelectric generators
Solar energy utilization
Evacuated tube solar collectors
Commercial used

ABSTRACT

Solar thermoelectric generator (STEG) systems are attractive because they can convert solar heat directly into electricity via solid-state thermoelectric generators. Nevertheless, its low energy conversion efficiency has prevented it from wide-scale implementation and commercialization. To date, the best experimental efficiency for STEG without concentrated is 4.6%, and only testing single thermoelectric unicouple within a specific application deployment context. In this paper, a mathematical model containing various heat losses ignored by previous studies are developed and validated to confirm the possibility of improved STEG performance. We developed a high-performance solar thermoelectric hybrid device composed of heat pipe evacuated tubular collector, solar selective absorber, and TE modules by conducting a comprehensive optimization in terms of thermoelectric material, the optical and thermal efficiency of solar selective absorber, heat management and device integration. The experimental results show that the thermoelectric conversion efficiency of proposed device was enhanced significantly, it produced a peak electrical efficiency of 5.2%. And the residual solar energy is stored for either power generation or domestic used. The peak exergy efficiency of the system reached up to 7.17%. The efficiency is higher than the previously reported best value. We experimentally demonstrated the feasible of the scale application of solar thermoelectric generators. And the results indicated that STEG system is a promising alternative solar energy thermal utilization technology in the small scale co-generation applications.

1. Introduction

With the rapidly industrial and economic development, the problems related to environment and energy gradually drew worldwide attentions. How to solve these problems is a major global challenge of the world [1]. Solar energy utilization is a promising choice to solve it. There are many technologies available to harvest solar energy, the two main of those are solar photovoltaic [2] and solar thermal conversion processes [3–5]. Photovoltaic process can convert some of the spectrum directly into electricity, while solar thermal processes convert solar energy into heat and utilize this heat for power generation by mechanical heat engines [6–8].

Being no moving parts, no chemical reactions, environment friendly, silent, and reliable, thermoelectric generator (TEG) is emerging as a promising alternative way of utilizing solar heat [9]. It gains significant renewed interest in the field of solar energy, known as solar thermoelectric generators (STEGs) [10]. Unlike the existing solar thermal conversion processes, STEGs are solid devices with no mechanical or moving parts. Since the TEGs is composed of two type of thermocouples in series and in parallel, the STEGs is stretchable. Compared with PV technology, STEGs can almost utilize all of the solar spectrum while PV technology can only use the fraction of spectrum above the bandgap, allowing for higher energy conversion efficiency. Although the first concept for a STEG was proposed in 1888 and it has been developed for more than one century [11,12], the low energy-conversion efficiency and/or complicated and bulky designs have prevented its application and commercialization [13]. During this period, a lot of research work including theoretical and experimental research was carried out to improve the efficiency of thermoelectric generators. The first documented detailed study for a STEG was published in 1954 by Telkes [14]. The maximum efficiency achieved of a flat-panel STEG was 0.63%. After that, early work [14–18] showed low conversion efficiency almost $< 1\%$ due to thermoelectric materials with low conversion efficiency and low hot-side temperature, And STEGs have been

* Corresponding author.
E-mail address: hwei@hfut.edu.cn (W. He).

https://doi.org/10.1016/j.enconman.2019.05.089
Received 10 February 2019; Received in revised form 21 May 2019; Accepted 26 May 2019
Available online 06 June 2019
0196-8904/

Table 1
Previous study results for STEG before 2011.

System and composition	Conditions	Efficiency	Year	Author
ZnSb alloys & Bi alloy	1 × sun	0.63%	1954	Telkes [14]
Bi_2Te_3 alloys	1 × sun	< 1%	1980	Goldsmid [15]
Bi_2Te_3 alloys	1 × sun	< 1%	1982	Dent and Cobble [19]
Commercial Bi_2Te_3 thermoelectric module	1 × sun	0.85%	1998	Omer [17]
Commercial Thermoelectric module	1 × sun	0.65%-1.1%	1999	Rockendorf [20]
Commercial Thermoelectric module	low concentration	< 1%	2005	Vatcharasathien [16]

designed and optimized for space applications, and none of earth-based STEGs made significant improvement over Telkes' work. Table 1 summarizes the previously published experimental results for different solar thermoelectrics.

Until 2011, Kraemer et al. [10] set a new efficiency record for STEG by using a selective absorber and advanced Bi_2Te_3 based nanocomposites. And the experimental work on STEG technology showed promising results for large-scale and potentially cost-effective deployment on rooftops or for the integration in solar hot water systems. Chen et al. [10,21] modeling of the solar thermoelectric generators. The results showed STEGs can have attractive efficiency with little or no optical concentration working in the low temperature range (150–250 °C) by operating in an evacuated environment. In 2012, He et al. [22] proposed a vacuum tube solar heat pipe system combined with a thermoelectric generator for water heating and electric power. The experimental prototype unit showed 1% electrical efficiency for the solar irradiance of 700 W/m^2 and the ambient temperature of 20 °C. In 2013, Miao et al. [23] designed a pilot solar STECG system. But for thermoelectric modules with ZTM = 1, when the solar insolation, wind velocity, ambient temperature and water temperature are 1000 W/m^2, 1.3 m/s, 25 °C and 25 °C, respectively, the electrical efficiency is only 1.59%. In 2016, Li et al. [24] proposed the conceptual development and theoretical analysis of a solar collector-incorporated thermoelectric generation which could generate both electricity and hot water. The thermal efficiency of the system could be reach up to 57.35% and the electrical efficiency up to 0.58% under the solar radiation intensity of 600 W/m^2. In 2017, Lv et al. [25] optimized He's design [22] by using the flat-plate heat pipes that are more efficient in contact with thermoelectric modules. It also reduces contact thermal resistance and heat loss, increases the power generation efficiency of the STEG system to 3.0%, and is equal to the electrical efficiency (3–4%) of the organic low temperature Rankine cycle system.

However, To date, the best experimental efficiency for STEG without concentrated is 4.6% et al. [10], and only testing single thermoelectric unicouple within a specific application deployment context. Most previous studies were theoretical or small-scale validation experiments used thermoelectric monomers or single modules [10,25–29]. Furthermore, scale solar thermal applications of STEG has not yet been proven [30,31] and the efficiency of these designs is so low that they cannot be scaled up. Up to now, STEGs is still debated its applicability for scale implementation [30].

Based on the above discussion, realizing a high-performance and large-scale STEG system (STEGs) would be a significant contribution. In the present work, we constructed and tested a novel high-performance STEGs without optical concentration. Four key parts have been improved throughout the system: (1) high performance thermoelectric materials matching the temperature of collector, (2) high performance selective coating and (3) optimization of TE devices by filling the insulating and (4) the use of radiation-reducing shield. As a result, a new record experimental efficiency of 5.2% at a normal solar irradiance of 1000 W/m^2 was found. And the cogeneration system have been proved to provide electricity and heat simultaneously and economically. Small-scale solar thermoelectric applications has been developed and its applicability for wide-scale implementation has been proved. In addition, this work has developed a mathematical model containing various heat losses that analyzes the performance of STEG in cogeneration applications and validates the thermodynamic model by establishing experimental prototypes, confirming the possibility of improved STEG performance. The previous assessments of STEG were based on the first law of thermodynamics. Since the essence of energy utilization is to extract as much available energy as possible, these assessments cannot perfectly assess the performance of the STEG. Thus, evaluating STEG based on the second law of thermodynamics is conducted, which revealed a system with a reasonable degree of energy. It provides guidance and advice for system optimization and improvement. The details are discussed in the following sections.

2. Model

The design of a STEG unit as shown in Fig. 1. It consists of solar collecting system and thermoelectric power generation system. One major challenge in the STEG system is to create a significant temperature difference across the TE module. Thus, for a high electric power conversion efficiency, all solar heat were supposed to be conducted over the TE module.

Some assumptions were made in the modeling:

(1) The temperature of selective surface maintained constant and uniform with the help of superconducting heat pipe, and so did the hot side temperature of the TE elements.
(2) The properties of thermoelectric materials are independent of temperature for the systems operated in a small temperature range [32].
(3) Electrical and thermal contact resistances are negligible.

The energy balance equation for the solar absorber surface can be written as:

$$\tau_g \alpha_s C_{th} q_s A_s = Q_h + \varepsilon_{ss}\sigma A_s (T_h^4 - T_a^4) + \varepsilon_{hc}\sigma (A_s - A_{teg})(T_h^4 - T_c^4) + E_{b3} + E_{b4} + h_{conv,h-a}(A_s - A_{teg})(T_h - T_c) + Q_{con} \quad (1)$$

where q_s is the solar insolation per unit area, τ_g is the transmittance of the glass tube, α_s is the absorptance of the selective surface, C_{th} is thermal concentration ratio which is similar to optical concentration [25], ε_{ss} is the effective emittance between the selective surface and the ambient, ε_{hc} is the emittance between the hot side and the cold side of TE. E_{b3} and E_{b4} are the radiative and convective heat losses e of TE module respectively. Q_h is the heat flow from the TEG to the cold side. A_s is the selective surface are and A_{teg} is the cross section area of TEG module.

The left side of the equation is the solar energy input. The first term at right side of equation is the heat conducted to the hot side of TE module, second and third term represents the radiative and convective heat losses from absorber surface to ambient respectively, and the fourth and last term represents heat losses of TE module. In order to diminish the radiative and convective heat losses within the TE module, insulating materials fill the gaps between n-type and p-type thermoelectric materials. The heat loss of the solar absorber and thermal concentrator by air convection is eliminated by enclosing it inside a

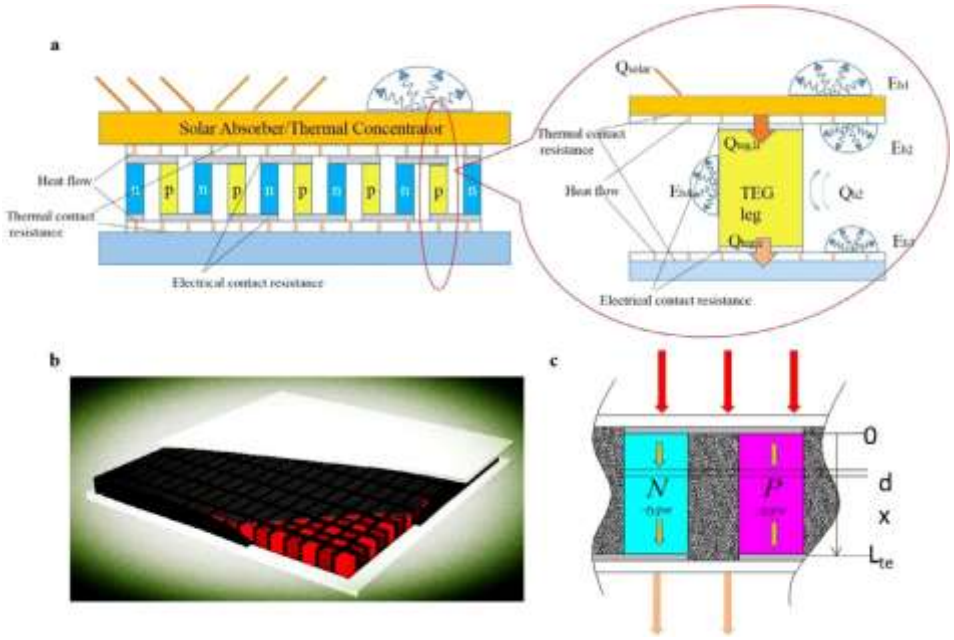

Fig. 1. Schematic of a STEG and thermoelectric (TE) elements for numerical simulation of TE device. a, Energy balance, b, TE device with adiabatic fillers. c, Discretization of thermoelectric (TE) elements for numerical simulation of STEG.

vacuum tube [33]. Thus, we neglect convective heat losses from absorber surface to outside ambient and the radiative and convective heat losses related to TEG module in the right side of Eq. (1), such that Eq. (1) becomes:

$$\tau_g \alpha_s C_{th} q_s A_s = Q_h + \varepsilon_{ss} \sigma A_s (T_h^4 - T_a^4) + Q_{con} \tag{2}$$

Q_{con} is the conduction and convection loss determined by the filling quality and the thermal conduction of the filling materials.

Now, the heat leaving the absorber's surface via the TE module can be expressed as:

$$Q_h = SIT_h + K(T_h - T_c) - \frac{1}{2}I^2R_i - \frac{\mu I (T_h - T_c)}{2} \tag{3}$$

$$Q_c = SIT_c + K(T_h - T_c) + \frac{1}{2}I^2R_i + \frac{\mu I (T_h - T_c)}{2} \tag{4}$$

where S is the Seebeck coefficients of the thermoelectric materials, I is the current flowing through the thermoelectric elements, K and R_i are the thermal conductivity and electrical resistances, respectively.

$$S = N(S_p - S_n) \tag{5}$$

$$K = N(K_n + K_p);\ K_p = \frac{k_p A_p}{L_p},\ K_n = \frac{k_n A_n}{L_n} \tag{6}$$

$$R = N(R_n + R_p);\ R_p = \frac{\rho_p A_p}{L_p},\ R_n = \frac{\rho_n A_n}{L_n} \tag{7}$$

where A and L represents cross-sectional area and the length of the p-type and n-type thermoelectric elements, respectively.

The electrical output of the STEG can be expressed as follows:

$$P_e = I[N(S_p - S_n)(T_h - T_c) - IR_i] \tag{8}$$

The electrical output of the STEG can be expressed as follows:

$$P_{out} = I^2R_{load} = \frac{[N(S_p - S_n)(T_h - T_c) - IR_i]^2 R_{load}}{[N(R_n + R_p) + R_{load}]^2} \tag{9}$$

where R_{load} is the load resistance.

Differentiating Eq. (9), that is,

$$\frac{dP}{dR_{load}} = 0 \tag{10}$$

Rearranging Eq. (10) gives:

$$R_{load} = \frac{N(R_n + R_p)}{1 - \frac{4N(R_n + R_p)}{\Delta T}\frac{d\Delta T}{dR_{load}}} \tag{11}$$

which represents external resistance for maximum output power.

The efficiency of the STEG unit can be expressed as follows:

$$\eta_e = \frac{P_{out}}{Q_{in}} = \frac{S(T_h - T_c)I - I^2R - \mu I(T_h - T_c)}{C_{th} q_s A_s} \tag{12}$$

The efficiency of STEG can also be written as follows:

$$\eta_e = \frac{Q_h}{C_{th} q_s A_s} \times \frac{P_{out}}{Q_h} = \eta_{ot}\eta_{te} \tag{13}$$

If the heat rejected at the cold side of TE module could be collected, the energy efficiency of cogeneration system can be expressed as:

$$\eta_{system} = \frac{S(T_h - T_c)I - I^2R - \mu I(T_h - T_c) + Q_{re}}{C_{th} q_s A_s} \tag{14}$$

Earlier assessments of STEG were based on the first law of thermodynamics. Since the essence of energy utilization is to extract as much available energy as possible, these assessments cannot perfectly assess the performance of the STEG. Thus, evaluating STEG based on the second law of thermodynamics is necessary, which revealed a system with a reasonable degree of energy.

To find the exergy efficiency of STEG, the exergy input of the solar radiation has to be found out which is given by Petela [34]. If the output of STEG is the electricity which is pure exergy. The exergy efficiency of the STEG can be expressed as:

$$\Psi_e = \frac{P_e}{Ex_{in}} = \frac{S(T_h - T_c)I - I^2R - \mu I(T_h - T_c)}{Q_{in}\left(1 - \frac{4}{3}\frac{T_a}{T_{sun}} + \frac{1}{3}\left(\frac{T_a}{T_{sun}}\right)^4\right)} \tag{15}$$

Similarly, if the heat rejected at the cold side of TE module are collected and used for power generation instead of space heating or domestic hot water, the exergy of the waste heat has to be found out which is given by [35]. And the exergy efficiency of cogeneration

system can be expressed as:

$$\Psi_e = \frac{P_e + P_{re}}{Ex_{in}} = \frac{S(T_h - T_c)I - I^2R - \mu I(T_h - T_c) + \dot{m}C_p\left(T_{out} - T_{in} - T_a \ln\frac{T_{out}}{T_{in}}\right)}{Q_{in}\left(1 - \frac{4}{3}\frac{T_a}{T_{sun}} + \frac{1}{3}\left(\frac{T_a}{T_{sun}}\right)^4\right)} \quad (16)$$

3. Design and fabrication

The STEG systems are composed of:

(a) High efficiency Bi_2Te_3-based modules for thermoelectric power generation between 100 and 300 °C. This high efficiency thermoelectric module depends on high performance p-type Bi_2Te_3-based thermoelectric materials with their properties given in [36]. Those n–p Bi_2Te_3-based materials are fabricated to five prototype TE modules. The dimensions of p-n type thermoelectric element are $1.5 \times 1.5 \times 1.7$ mm^3. 71 pairs of p–n type element were assembled in series or in parallel with the ceramic substrates as the electrically isolated foundation. Aerogel are selected as insulating materials to fill the gaps in TE module.

(b) High-performance wavelength-selective solar absorbers, a wavelength-selective selective absorbers with exceptionally low emissivity in the thermal wavelength range and high visible absorptivity for the solar spectrum was used in our system (provide by Beijin Jintaiyang Co., Ltd.). The properties of solar absorber coating and test results are shown in Fig. 2. The results shows that the surface temperature can be reached 300 °C even without optical concentration, which matched with the optimal operation temperature T_h of our Bi_2Te_3-based materials.

(c) An innovative design that uses a high thermal concentration by lateral heat conduction within the highly thermally conductive absorber substrate such as superconducting heat pipes. This method of concentrating heat has been used in various thermal systems [10,37]. The higher the absorptance and high thermal concentration, the higher operating temperature. Following Kirchhoff's law of thermal radiation, the high temperature caused large radiation heat loss [38]. Thus, an aluminum heat shield is add below the absorber to reduce radiation heat loss caused by thermal concentration and improve the thermal performance of it in a cost-effective manner [39].

Our experimental system is illustrated in Fig. 3a. Five devices were fabricated, and a systematically optimized process and integration techniques were used to make them to be portable like domestic solar collectors. It can be used on flat ground or residential and commercial rooftops depends on users' wishes. Moreover, as is shown in Fig. 3c the STEG unit in which the solar selective absorption coating is directly applied to the thermal end of the fabricated prototype TE modules ($C_{th} = 1$) also fabricated as contrast group for comparison to put on the bench.

4. Performance

Fig. 4b and c show the performance of our fabricated STEGs under a solar simulator around solar irradiance of 1 kW/m^2 corresponding to AM1.5G. When the cold side is maintained at 20 °C, the electrical efficiency of the STEG system reached up to a record-high efficiency of 5.2%, which is almost twice as efficient as Telkes' best device. The STEG power output reaches 5.3 W. More than 10 similar units and 100 repeated experiments have been tested and routinely achieved an efficiency in the range 5.0–5.2% around AM1.5G conditions. Meanwhile, A MATLAB code written based on the thermodynamic model above was also carried out for the same condition as the experiment. In order to better match the results of the experiment, an electrical resistance of 1.02Ω is included to replace contact loss. The results of efficiency, power output, and I–V characteristics were shown in Fig. 4. The conventional TEG system is a constant temperature difference system while our STEG system is a constant heat input system. It also validates the Eq. (11). It can be seen that the efficiency of STEGs first increases and then decreases. Thus, there is an optimal solar irradiance for a given TE module. The phenomenon can be explained as: when the solar absorber is at a lower temperature. Thus, the output efficiency of STEG is low because of the smaller temperature difference between TE modules. At this time, the emissivity is also very low. With the increase of high solar radiation, the thermal efficiency grows fast firstly and then have descendent tendency as the solar radiation continue to rise. If the thermal concentration is too high, the temperature reached too high, the radiation loss is high, the increase of irradiation intensity has more influence on radiation loss. In addition, when the temperature exceeds the best working temperature of the thermoelectric materials, resulting in a decrease in STEG efficiency. And as is shown in Fig. 4f, the exergy efficiency shows some same development tendencies, such as it increased firstly and then decreased when solar radiation increases. It is clear from both the figures that there is a solar irradiance at which both energy and exergy efficiencies are maximum, such as the peak exergy efficiency of the system is as high as 7.17% at the solar irradiance of 1032 W/m^2 and a peak output efficiency of 5.2% at the solar irradiance of 1021 W/m^2, which can be obtained from the figures or equations. Further, the exergy efficiency is higher than the energy efficiency because of lesser exergy content in input solar heat, and the overall exergy efficiency is considerable when considering the exergy efficiency of waste heat.

The measured efficiency changed with solar irradiance are shown in Fig. 4d. The STEG will perform at its peak under optimal conditions.

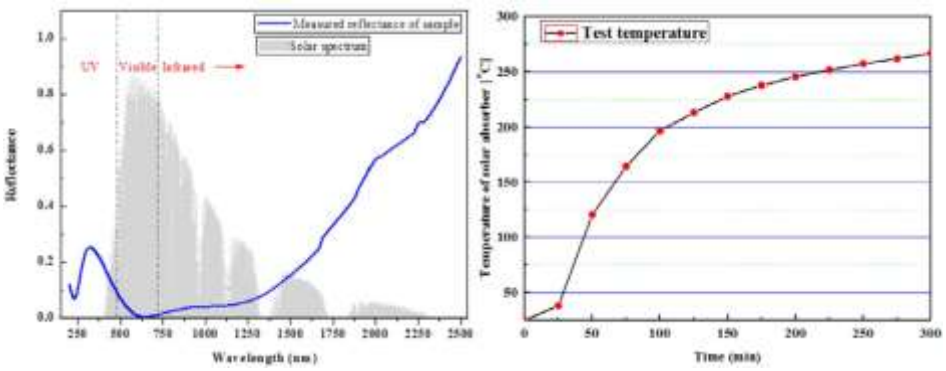

Fig. 2. The properties of solar absorber coating and test results. a, The properties of solar absorber coating, b, Test temperature of the coating under 800 W/m^2 Solar Irradiation.

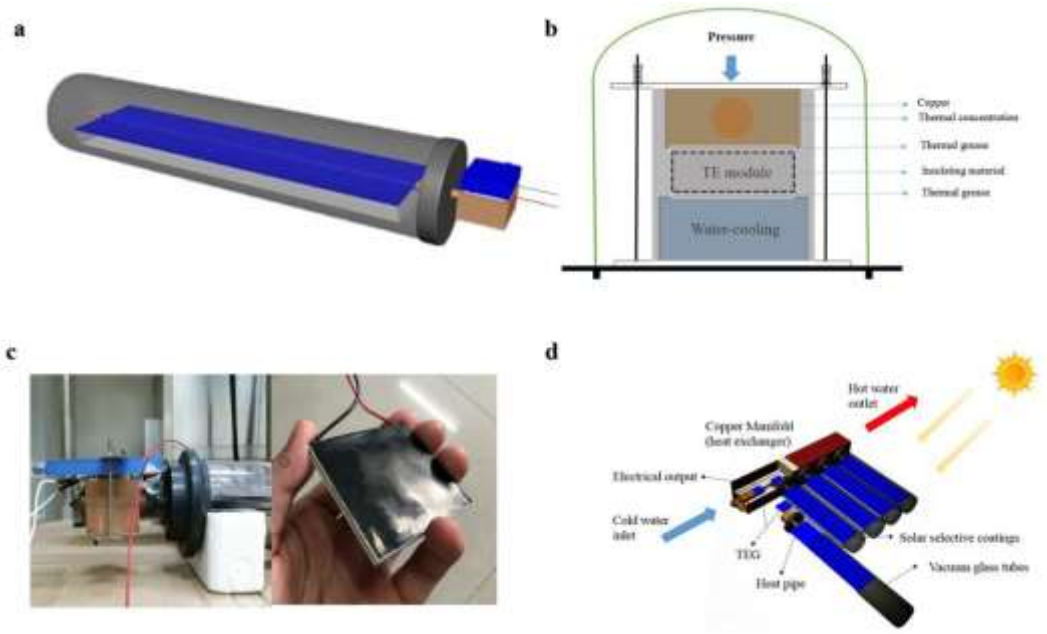

Fig. 3. Design and fabrication of STEGs. a, Schematic of a STEG unit, b, A schematic diagram of the combination of solar collector and TE. c, Fabricated STEG assembly and photos of key parts. d, the STEG system.

However, one of the major challenges of solar technologies is the varying ambient conditions over the course of a day and a year. The effects of changing ambient conditions on the STEG performance are illustrated in Fig. 4. From Fig. 4b–d, and f, we know that the external resistance for maximum output power of STEG system and that of conventional TE device are different because of different input conditions. As is shown in Fig. 4c, it is clear that the high solar radiation responds to the high absorber temperature. The STEG performances peak at solar irradiances of approximately 1000 kW m^{-2} and the STEGs operate with an absorber temperature of 270–290 °C which also matches the best operated temperature of our TE materials. And at this time the STEG efficiency is also up to the highest (Fig. 4c, d). It can be seen that there is an optimal thermal concentration for a given solar intensity and size of the STEG. The solar intensity varies over the course of a day even when the sun is partially blocked by clouds. A decrease of 100 W/m^2 in the solar flux density, the drop in the STEG efficiency is less than 20%, which is smaller than a purely thermally concentrating STEG in previous study [23]. The STEGs is the delayed thermal response resulting from the heat pipe vacuum tube.

Comparison with previous work, besides borrowing previous experience such as: the use of selective surface, the combination with heat pipe vacuum tube and operation the STEG in a vacuum environment. There are several points that improved efficiency: (1) high performance thermoelectric materials matching the temperature of collector, (2) high performance selective coating and (3) optimization of TE devices to decrease the heat loss of the module by filling the insulating and (4) the use of radiation-reducing shield in the solar collector. The effective ZT of the thermoelectric materials we used at optimal operation conditions is 1.03, averaged ZT values of up to 0.8 between 100 and 300 °C. Even though the performance of our system is no better than STEGs with high optical solar concentration, it is still a remarkable improvement for STEG without optical solar concentration over previous reports [10,20,28,37], as is shown in Fig. 5. Fig. 5b shows simulations and experiments carried out for a STEG module which the solar selective absorption coating is directly applied to the hot end of the fabricated prototype TE module (the thermal concentration is equal to 1) to demonstrate the impact of these improvement. Generally speaking the simulated performance results are in good agreement with the experimental results. The small discrepancy between modeling and experimental results can be attributed to the uncertainties of the some properties in simulation. For example, the effective TE device ZT is substantially lower compared to the TE material ZT due to experimental imperfections such as contact resistances and thermal loss in the bond part. However, the record-high STEG efficiencies demonstrated here at solar irradiances about 1000 W/m^2 are still 2 times higher compared to best values of previously reported. Thus, most economically and likely to operate in practice. And the four key design features enable a stable and efficient STEG operation with much larger operating time and operation in a real environment. So, our devices are most likely to be used in practice for residential and commercial rooftops.

5. Economy

Ultimately, the value of any new technology is determined not only by efficiency but also by cost. Although our collector is specially processed, it will be cheap by manufacturing on a large scale after finalizing the design. By 2017, the annual production of solar collectors had exceeded 30 million m^2 and the total installation area had reached 150 million m^2 [40,41]. As a consequence of this mass production, the cost heat pipe based solar collectors is decreasing year by year, widely available and of good quality. STEGs made from the heat-pipe vacuum tube solar collector with integrated TE are easy to fabricate and only slightly more expensive than solar collectors on their own [42]. Compared to the existing solar water heating systems, the price of our STEG system is mainly determined by the cost of TE module. The cost for the TE modules can be estimated by the cost of its materials. The prototype TE modules are fabricated by n–p Bi_2Te_3-based materials. A commercially available hot extruded Bi_2Te_3-based material was chosen as the n-type counterpart and $Bi_{0.5}Sb_{1.495}Cu_{0.005}Te_3$ were selected as the p-type materials. At the present, prices of the bismuth telluride and copper antimony based materials used, at the current price of approximately \$250 kg^{-1} Bi_2Te_3, the cost of the our TE material is approximately \$26 per kg or \$0.71 per electrical watt generated. The actual cost of modular manufacturing is certainly higher than this. The discrepancy is due to the cost of the assembly such as ceramic plates used to fabricate the TE module. The costs for heat exchangers of the TE device is another obstacle to cost reduction [43]. Fortunately, our system has overcome those problem. Furthermore, it should be acknowledged that the

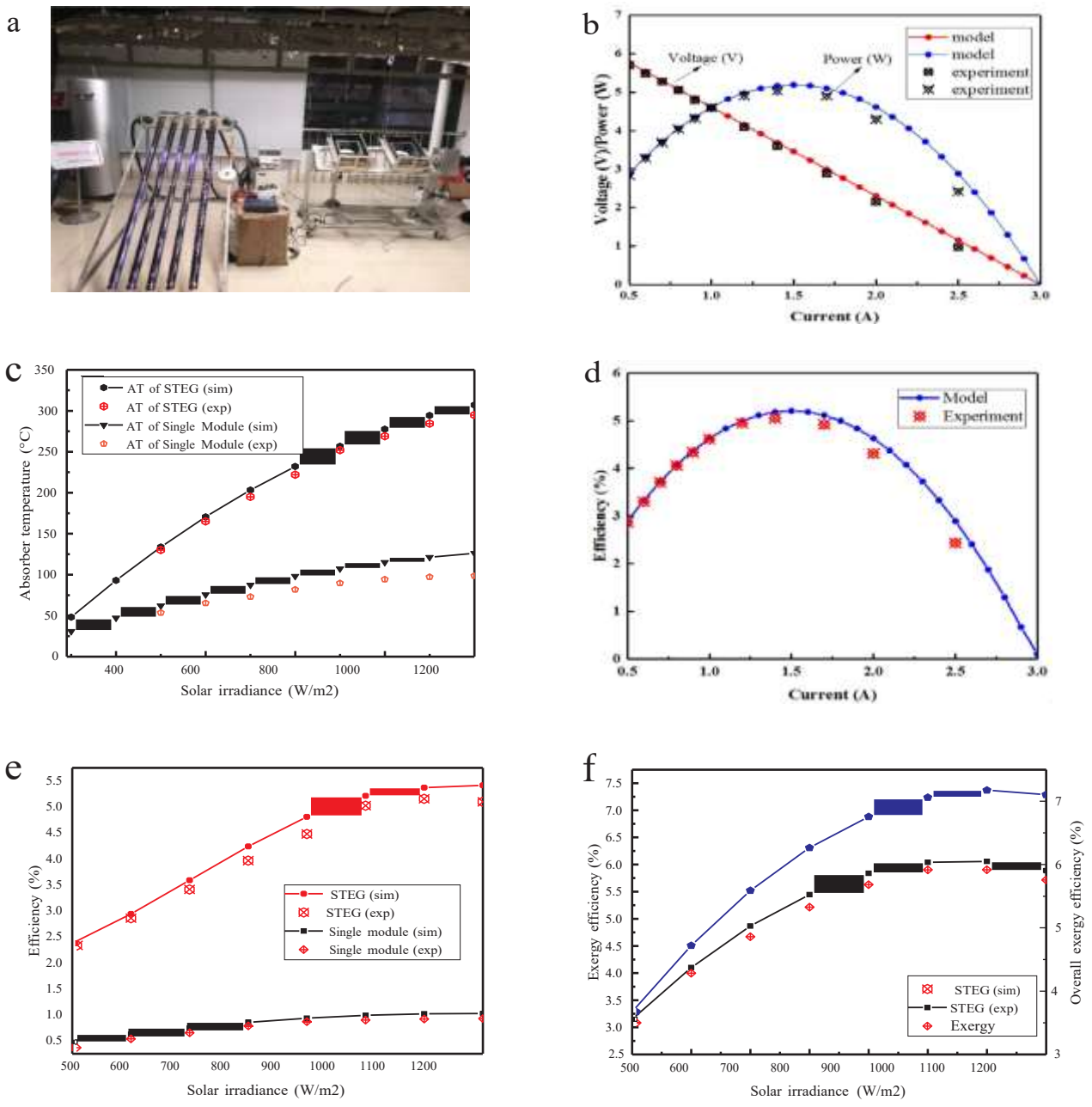

Fig. 4. The STEGs and their performance characteristics. Typical STEG unit characteristics at solar radiation of 1000 W/m^2. a, The STEGs. b, Electric characteristics of the STEGs. c, Absorber temperature. d, Efficiency as a function of the current. e, Efficiency as a function of the solar irradiance. f, Exergy efficiency as a function of the solar irradiance.

electricity efficiency of STEG of about 5–6% is 4–5 times lower than the efficiencies of existing solar panels. The waste heat rejected from TE cold side have be collected for heating water or space heating, to compensate for the low electrical efficiency and improve economy. Evacuated tube solar collectors are widely used in solar hot-water systems housing stock worldwide [42], especially in China. The water temperature is usually required in the range of 35–50 °C for domestic hot water according to Chinese solar water heating system design principle [22,33]. As is shown in Fig. 5a, the low cooling water temperature imply that with a small expense of its electric efficiency, Our STEG system can be used to obtain higher temperature waste heat to enhance the user experience and improve economy. We have confirmed that the system can achieve costs below $1/W if the waste heat rejected from TE cold side was taken into consideration.

The case study area is situated on the No.1 villa on the peninsula, in Hefei, China. Aerial views of the building under investigation are shown in Fig. 6b. The region is characterized by a Subtropical monsoon climate (2014–2016: 2.18 m/s). The intensity of solar radiation was taken as 800–1000 W/m^2, which corresponds to the direct normal irradiance (DNI) in Hefei, China, at 30° of northern latitude, at the summer time of the year. Fig. 5a depicts the building under study, the exterior spaces around them and the topography of the area. If 50% solar energy available area on the roof of the house is equipped with STEGs. Since the active surface area of the STEG unit was 0.114 m^2, 48 STEG units can be installed on the roof.

The results shows that our STEG system can generate 3.3 kWh of electrical power. If the STEGs works at the reported capacity over eight hours of good sun irradiation per day, it can meet 165% of a small house demand, which daily electricity consumption is approximately 2 kWh [44]. Furthermore, the solar thermal heat collected during this

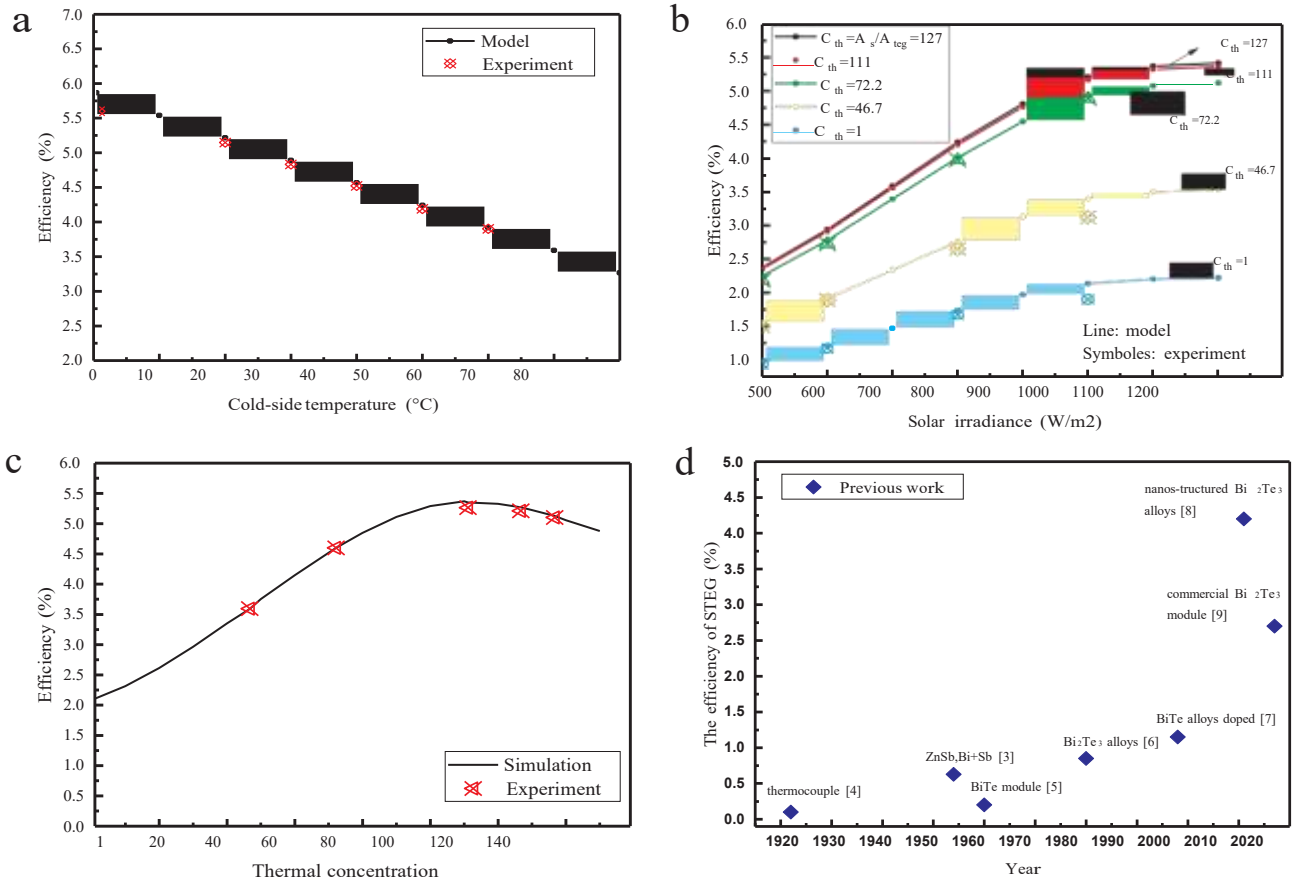

Fig. 5. Performance characteristics of the STEG under varying ambient conditions. Typical STEG unit characteristics at solar radiation of 1000 W/m^2. a, Efficiency vary with the cold-side temperature. b, Efficiency vary with solar radiation and typical C_{th}. c, Efficiency vary with the thermal concentration. d, Historical overview of experimental efficiency of STEGs without optical concentration.

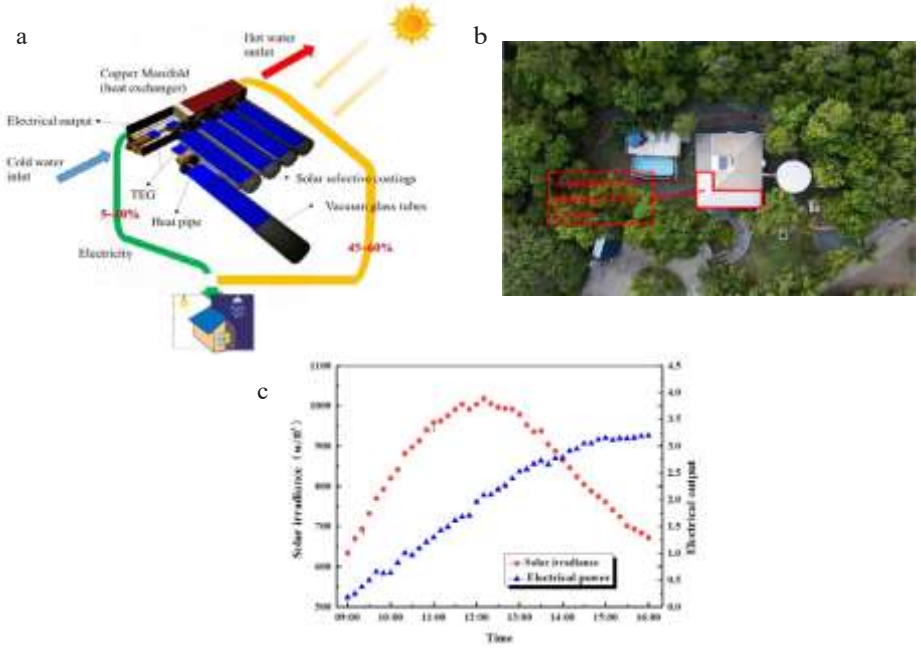

Fig. 6. Economy and case study. a, The STEG system for co-generation of electricity and hot water. b, Aerial views of the building under investigation, located at the No.1 villa on the peninsula, in Hefei, China. c, The variation of solar radiation and the corresponding output of the system in typical day.

period can provide an additional ~18.4 MJ (e.g. a 1 m^2 effective endothermic area operating at 40% thermal efficiency [20]), which would fulfill the entire domestic heat need for hot water or space heating, as is shown in Fig. 6. The results indicated that with further improvements in STEG system, it could fully satisfy the electrical and heating needs for the household.

6. Conclusion

In this work, a record high efficiency of a STEG system has been built and tested. The results show that our STEG system has many advantages and advanced points compare compared with previous work.

(1) Improve the efficiency of photo-thermal conversion, making high performance TE materials work in them optimum temperature ranges, optimizing thermoelectric devices and reduce the heat loss of each part. Those four key design features enable a stable and efficient STEG operation with much larger operating time and operation in a real environment. So, our devices are most likely to be used in practice for residential and commercial rooftops.
(2) In order to improve the performance of STEG, besides the development of materials with improved thermoelectric properties, future research directions should target further reduction of heat losses and improving contacts.
(3) TEG is compatible with popular used evacuated tube collector, indicating the potential of STEGs for co-generation of electricity and hot water, thus leading to improved system efficiency and economy.

This work demonstrated not only are STEGs growing into a competing alternative technology to the solar energy utilization, but they are also economical and simple to implement. And it could be suitable for real-world application. Large-scale experiments are now under way in house and rooftops to demonstrate the robustness and practicality of our solar thermoelectric co-generators under typical real-world conditions. This work gives hints for future improvement of the solar thermoelectric cogeneration system, and future research should focus not only on improving the TE materials efficiency and creating a new record but also on the practical application.

Declaration of Competing Interest

None.

Acknowledgments

The study was sponsored by the Fundamental Research Funds for the Central Universities (WK6030000071), the grants from Science and technology cooperation project of Qinghai Province (No. 2017-HZ-807), Beijing advanced innovation center for future urban design (No. UDC2016040200), and also Program for Dongguan Innovative Research Team Program (No. 2014607101008). We thank State Key Laboratory of High Performance Ceramics and Superfine Microstructure, Shanghai Institute of Ceramics, Chinese Academy of Sciences for their technical assistance with the thermoelectric materials and modules.

References

[1] Hussain A, Arif SM, Aslam M. Emerging renewable and sustainable energy technologies: state of the art. Renew Sustain Energy Rev 2017;71:12–28.
[2] Luque A, Hegedus S. Handbook of photovoltaic science and engineering. John Wiley & Sons; 2011.
[3] Duffie JA, Beckman WA. Solar engineering of thermal processes, Fourth Edition 2013.
[4] Muller-Steinhagen H, Trieb F. Concentrating solar power: a review of the technology. Ingenia 2004;18:43–50.
[5] Baharoon DA, Rahman HA, Wan ZWO, Fadhl SO. Historical development of concentrating solar power technologies to generate clean electricity efficiently – a review. Renew Sustain Energy Rev 2015;41:996–1027.
[6] Hu A, Levis S, Meehl GA, Han W, Washington WM, Oleson KW, et al. Impact of solar panels on global climate. Nat Clim Change 2015;6.
[7] Mills D. Advances in solar thermal electricity technology. Sol Energy 2004;76:19–31.
[8] Weinstein LA, Loomis J, Bhatia B, Bierman DM, Wang EN, Chen G. Concentrating solar power. Chem Rev 2015;115:12797–838.
[9] Snyder GJ, Toberer ES. Complex thermoelectric materials. Nat Mater 2008;7:105–14.
[10] Kraemer D, Poudel B, Feng HP, Caylor JC, Yu B, Yan X, et al. High-performance flat-panel solar thermoelectric generators with high thermal concentration. Nat Mater 2011;10:532.
[11] Everett J. The Thomson effect. Nature 1886;34:143.
[12] Heaviside O. Extension of Kelvin's thermoelectric theory. Nature 1903;68:78.
[13] Wood C. Materials for thermoelectric energy conversion. Rep Prog Phys 1988;51:459–539.
[14] Telkes M. Solar thermoelectric generators. J Appl Phys 1954;25:765.
[15] Goldsmid H, Giutronich J, Kaila M. Solar thermoelectric generation using bismuth telluride alloys. Sol Energy 1980;24:435–40.
[16] Vatcharasathien N, Hirunlabh J, Khedari J, Daguenet M. Design and analysis of solar thermoelectric power generation system. Int J Sustain Energy 2005;24:115–27.
[17] Omer S, Infield D. Design optimization of thermoelectric devices for solar power generation. Sol Energy Mater Sol Cells 1998;53:67–82.
[18] Xi H, Luo L, Fraisse G. Development and applications of solar-based thermoelectric technologies. Renew Sustain Energy Rev 2007;11:923–36.
[19] Dent C, Cobble M. A solar thermoelectric generator experiments and analysis. 4th international conference on thermoelectric energy conversion. 1982. p. 75–8.
[20] Rockendorf G, Sillmann R, Podlowski L, Litzenburger B. PV-hybrid and thermoelectric collectors. Sol Energy 1999;67:227–37.
[21] Chen G. Theoretical efficiency of solar thermoelectric energy generators. J Appl Phys 2011;109:104908.
[22] He W, Su Y, Wang YQ, Riffat SB, Ji J. A study on incorporation of thermoelectric modules with evacuated-tube heat-pipe solar collectors. Renewable Energy 2012;37:142–9.
[23] Zhang M, Miao L, Kang YP, Tanemura S, Fisher CAJ, Xu G, et al. Efficient, low-cost solar thermoelectric cogenerators comprising evacuated tubular solar collectors and thermoelectric modules. Appl Energy 2013;109:51–9.
[24] Li G, Ji J, Zhang G, He W, Chen X, Chen H. Performance analysis on a novel micro-channel heat pipe evacuated tube solar collector-incorporated thermoelectric generation. Int J Energy Res 2016;40:2117–27.
[25] Lv S, He W, Hu D, Zhu J, Li G, Chen H, et al. Study on a high-performance solar thermoelectric system for combined heat and power. Energy Convers Manage 2017;143:459–69.
[26] Severy ML. Apparatus for generating electricity by solar heat. US Patent A1894.
[27] Telkes M. Solar thermoelectric generators. J Appl Phys 1954;25:765–77.
[28] Amatya R, Ram RJ. Solar thermoelectric generator for micropower applications. J Electron Mater 2010;39:1735–40.
[29] Kraemer D, Jie Q, Mcenaney K, Cao F, Liu W, Weinstein LA, et al. Concentrating solar thermoelectric generators with a peak efficiency of 7.4%. Nat Energy 2016;1.
[30] Andrei V, Bethke K, Rademann K. Thermoelectricity in the context of renewable energy sources: joining forces instead of competing. Energy Environ Sci 2016;9:1528–32.
[31] Vining CB. An inconvenient truth about thermoelectrics. Nat Mater 2009;8:83–5.
[32] Baranowski LL, Snyder GJ, Toberer ES. Concentrated solar thermoelectric generators. Energy Environ Sci 2012;5:9055–67.
[33] Wang Z, Yang W, Qiu F, Zhang X, Zhao X. Solar water heating: from theory, application, marketing and research. Renew Sustain Energy Rev 2015;41:68–84.
[34] Petela R. Exergy of heat radiation. J Heat Transfer 1964;86:187.
[35] Chow TT, Pei G, Fong KF, Lin Z, Chan ALS, Ji J. Energy and exergy analysis of photovoltaic–thermal collector with and without glass cover. Appl Energy 2009;86:310–6.
[36] Hao F, Qiu P, Tang Y, Bai S, Xin T, Chu HS, et al. High efficiency Bi2Te3-based materials and devices for thermoelectric power generation between 100 and 300 °C. Energy Environ Sci 2016;9.
[37] Telkes M. Solar thermoelectric generators. J Appl Phys 2004;25:765–77.
[38] Incropera FP. Fundamentals of heat and mass transfer. Wiley; 1985.
[39] Zhang X, You S, Ge H, Gao Y, Xu W, Wang M, et al. Thermal performance of direct-flow coaxial evacuated-tube solar collectors with and without a heat shield. Energy Convers Manage 2014;84:80–7.
[40] REN21. Renewables 2017 GSR, 2017.
[41] Urban F, Geall S, Wang Y. Solar PV and solar water heaters in China: different pathways to low carbon energy. Renew Sustain Energy Rev 2016;64:531–42.
[42] Chopra K, Tyagi V, Pandey A, Sari A. Global advancement on experimental and thermal analysis of evacuated tube collector with and without heat pipe systems and possible applications. Appl Energy 2018;228:351–89.
[43] Leblanc S, Yee SK, Scullin ML, Dames C, Goodson KE. Material and manufacturing cost considerations for thermoelectrics. Renew Sustain Energy Rev 2014;32:313–27.
[44] Sundarraj P, Maity D, Roy SS, Taylor RA. Recent advances in thermoelectric materials and solar thermoelectric generators — a critical review. RSC Adv 2015;46:46860–74.